

## **Supplementary Materials**

### **Supplementary methods and materials**

#### **Mice and mating procedures**

Animal ethics approval was granted by the Guangdong Laboratory Animal Monitoring Institute (Guangdong, China). Mice were provided with chow and water in individually ventilated cages (IVC) under specific pathogen-free (SPF) conditions. The mice were housed under a 12 h light/night shift. For mating, heterozygous females were mated with hairless males. Offspring that shed hair after weaning were divided into cages (4–5 mice/cage). The control group consisted of ICR mice fed under the same conditions. The ICR and SHJH<sup>hr</sup> mice were a kind gift from Shanghai Jihui Animal Care Co., Ltd. (China).

#### **RNA extraction and transcription**

Tissue samples from the ICR and SHJH<sup>hr</sup> mice were homogenized in TRizol (Invitrogen, USA) using a homogenate instrument (Xiangyi, China). Total RNA was then extracted according to the operational guidelines. First-strand cDNA was synthesized using a thermocycler (Arktik, Thermo Scientific, USA) at 42 °C for 60 min and 75 °C for 15 min using a PrimeScript II 1<sup>st</sup> Strand cDNA Synthesis Kit (Takara, China). The cDNA product was stored in the refrigerator for polymerase chain reaction (PCR).

#### **PCR and primers**

PCR was performed according to the manual provided with Premix Taq Hot Start Version (Takara, China). The primers were synthesized by Sangon Biotech (Shanghai) Co., Ltd. (China). Primer sequence information is shown in Supplementary Table S3. The PCR procedure included three steps: i.e., denaturation at 98 °C for 10 s, annealing at 60 °C for 30 s, and elongation at 72 °C for 3 min, with 35 cycles. The PCR product was separated by electrophoresis in 1.0% agarose gel, with the bands used for DNA sequencing (Sangon Biotech (Shanghai) Co., Ltd., China). The DNA information of the PCR products was aligned using SnapGene v3.2.1 software (USA) and mutant sites were searched.

### **Histological analysis**

The mice were anesthetized with CO<sub>2</sub> and blood was collected. The heart was then perfused with saline solution. Thyroid and other tissues were removed, dissected, and rinsed in 4% paraformaldehyde (PFA, Sigma, USA) for 24 h. The tissues were dehydrated, hyalinized (Leica ASP300S, Germany), and embedded in wax blocks. The blocks were cut in 5 μM sections, which were then stained with hematoxylin and eosin (H&E) (Leica SV5030, German). The stained sections were scanned and analyzed using Aperio ImageScope v12.4.3 software (Leica, Germany). Finally, images were combined using Adobe Illustrator. Follicle structure analyses were performed with ImageJ software (National Institutes of Health, USA) as described previously (Kero et al., 2007; Ock et al., 2013). Using six slides each from the ICR and SHJH<sup>hr</sup> groups, 30 thyroid follicles were analyzed, follicle lumen area (colloid-containing area), whole follicle area, and number of visible nuclei per follicle were measured, and thyrocyte area (whole follicle area minus colloid area) and average thyrocyte area (thyrocyte area divided by number of visible nuclei) were quantified.

### **Mouse metabolism detection**

Metabolic rate was determined using a metabolic cage (L-DX) (Suzhou Junsheng Experimental Animal Equipment Co., Ltd., China). Firstly, the mice were placed in metabolic cages to acclimate for 3 days, after which the cages were cleaned, and chow and water were removed. On the fourth day, chow and water were weighed and placed in the cage. After 24 h, the remaining food and water, as well as mouse feces and urine, were removed and weighed. The process was then repeated and measured again. Finally, the weight of the chow, water, feces, and urine each day were analyzed for each mouse.

### **Heart rate and blood pressure**

A blood pressure monitor (BP-2010A series, Softron Biotechnology Co., Ltd., Japan) was used to measure the heart rate and blood pressure of the mice, as per the manufacturer's manual. Briefly, the computer was first connected to the software (BPTERM10AU, Japan), then the mice were placed in a mouse bag and their tails

were passed through the pressure sensor. Measurements were taken when the software interface displayed stable waves, i.e., mice were in a stable state. Measurements were recorded and mean index values for each mouse were obtained from three replicates.

### **Determination of TSH, T3, and T4 levels**

Mouse TSH, T3, and T4 ELISA kits were purchased from Shanghai Enzyme-linked Biotechnology Co., Ltd. (China). Serum TSH, T3, and T4 levels were measured according to the manufacturer's instructions. In brief, we added mouse serum or standard samples to the wells of a microtiter plate pre-coated with antibodies, then added antibody-labeled biotin and sealed the wells with a membrane at 37°C for 1 hour. The plate was then washed in a washing machine (Bio-Rad 1575, USA), after which we added horseradish peroxidase (HRP)-antibody at 37°C for 30 min. The plate was again washed in the washing machine, and an A and B mixture was added for development for 10 min. Finally, we added stop buffer and used a Multiskan Microplate Reader (Thermo Fisher, USA) to detect OD450.

### **Statistical analysis**

Results are presented as mean±standard error of the mean (SEM). Statistical analysis was performed using GraphPad v7.0 (USA) with Student's *t*-test or analysis of variance (ANOVA) with Tukey's *post hoc* test. A *P*-value of less than 0.05 was considered statistically significant.

## **REFERENCES**

- Ahmad W, Panteleyev AA, Christiano AM. 1999. The molecular basis of congenital atrichia in humans and mice: mutations in the hairless gene. *Journal of Investigative Dermatology Symposium Proceedings*, **4**(3): 240–243.
- Brancaz MV, Iratni R, Morrison A, Mancini SJC, Marche P, Sundberg J, et al. 2004. A new allele of the mouse hairless gene interferes with *Hox/LacZ* transgene regulation in hair follicle primordia. *Experimental and Molecular Pathology*, **76**(2): 173–181.
- Cachón-González MB, San-José I, Cano A, Vega JA, García N, Freeman T, et al. 1999. The *hairless* gene of the mouse: relationship of phenotypic effects with expression profile and genotype. *Developmental Dynamics*, **216**(2): 113–126.
- Kero J, Ahmed K, Wettschureck N, Tunaru S, Wintermantel T, Greiner E, et al. 2007. Thyrocyte-specific  $G_q/G_{11}$  deficiency impairs thyroid function and prevents goiter development. *The Journal of Clinical Investigation*, **117**(9): 2399–2407.
- Ock S, Ahn J, Lee SH, Kang H, Offermanns S, Ahn HY, et al. 2013. IGF-1 receptor deficiency in thyrocytes

impairs thyroid hormone secretion and completely inhibits TSH-stimulated goiter. *The FASEB Journal*, **27**(12): 4899–4908.

Panteleyev AA, Ahmad W, Malashenko AM, Ignatieva EL, Paus R, Sundberg JP, et al. 1998. Molecular basis for the rhino Yurlovo (*hrrhY*) phenotype: severe skin abnormalities and female reproductive defects associated with an insertion in the hairless gene. *Experimental Dermatology*, **7**(5): 281–288.

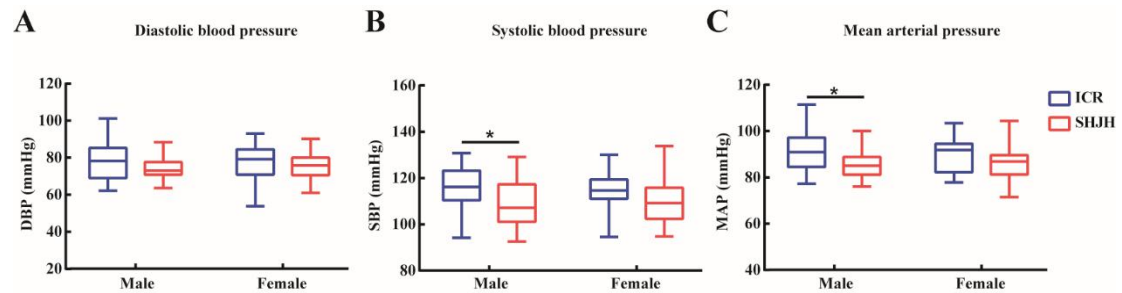
Tian M, Xiong YL, Wang WY, Zhang YP. 2004. Molecular genetic basis for the rhino mouse from Chinese KM subcolony. *Chinese Science Bulletin*, **49**(2): 146–152.

Zarach JM, Beaudoin III GMJ, Coulombe PA, Thompson CC. 2004. The co-repressor hairless has a role in epithelial cell differentiation in the skin. *Development*, **131**(17): 4189–4200.

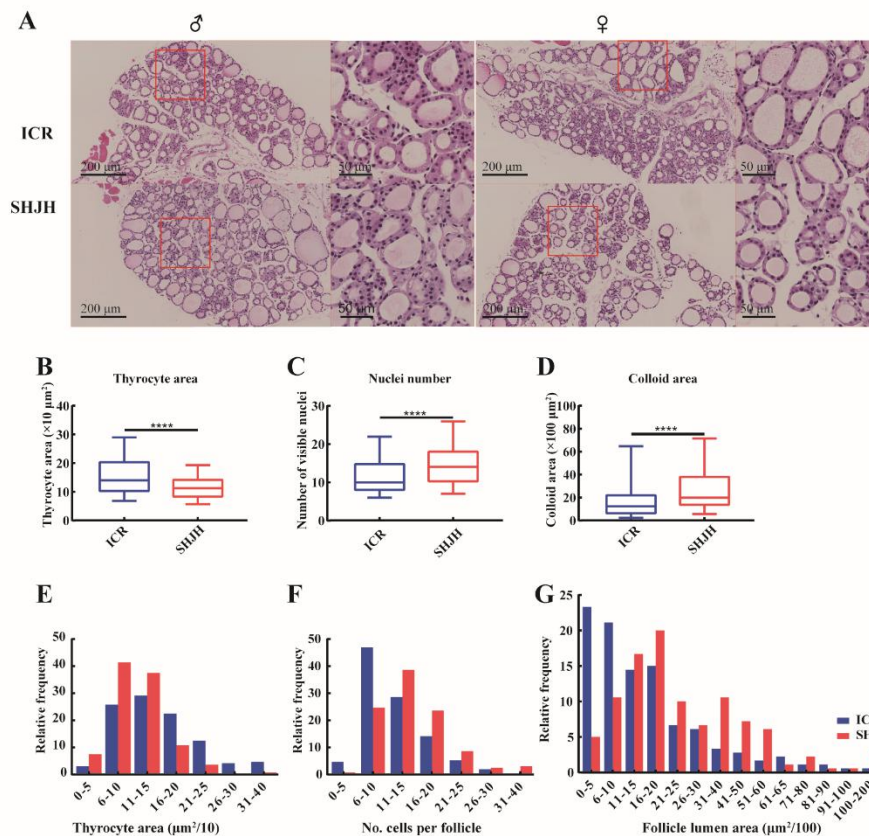
Zhang JT, Fang SG, Wang CY. 2005. A novel nonsense mutation and polymorphisms in the mouse hairless gene. *Journal of Investigative Dermatology*, **124**(6): 1200–1205.

Zhu KC, Xu CS, Zhang JT, Chen YY, Liu MD. 2017. Transgenic mice display hair loss and regrowth overexpressing mutant *Hr* gene. *Experimental Animals*, **66**(4): 379–386.

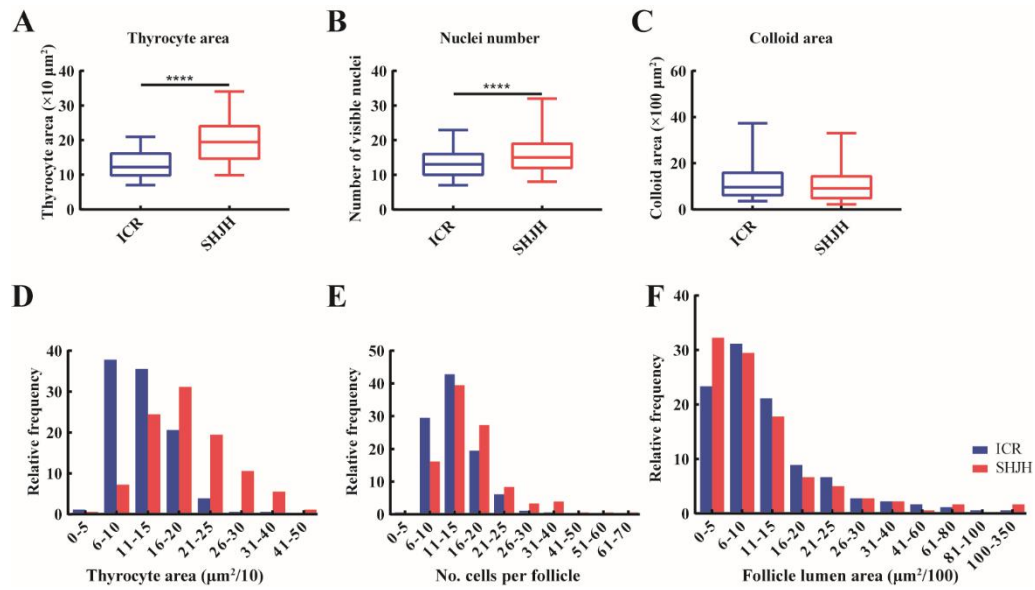
## Supplementary Figures and Tables



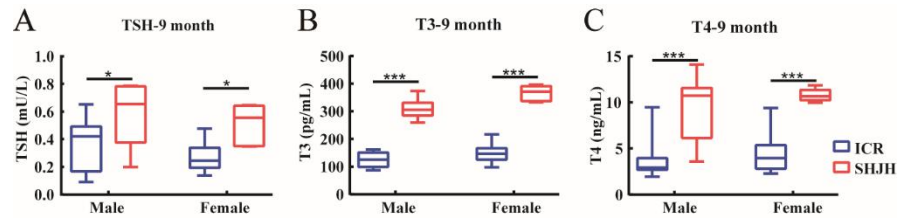
Supplementary **Figure S1. SHJH<sup>hr</sup> mice had lower blood pressure.** (A-C) DBP, SBP, and MAP of SHJH<sup>hr</sup> and ICR mice. Box plots in A and B represent 5<sup>th</sup> to 95<sup>th</sup> percentile, horizontal lines within boxes represent mean value, and error bars represent lowest and highest value in 5<sup>th</sup> percentile and 95<sup>th</sup> percentile, respectively. These data were measured using a noninvasive intelligent blood pressure meter three times for each mouse.  $n=18$  mice in each group. DBP, diastolic blood pressure. SBP, systolic blood pressure. MAP, mean arterial pressure. ICR, ICR mice; SHJH, SHJH<sup>hr</sup> mice. \* $P<0.05$ .



**Supplementary Figure S2. Thyroid follicle with smaller thyrocyte area in 8-week-old SHJH<sup>hr</sup> mice.** (A) H&E-stained thyroid section. Eight-week-old SHJH<sup>hr</sup> mice showed abnormal thyroid follicles with smaller thyrocyte area (B) and larger number of visible nuclei (C) and colloid area (D). (E-G) Relative frequency of thyrocyte area, number of cells per follicle (visible nuclei), and follicle lumen area (colloid area). Using six slides from each group, 30 thyroid follicles in each slide were randomly selected. Whole follicle area, visible nuclei per follicle, and follicle lumen area were measured, with thyrocyte area (follicle area minus follicle lumen area), average thyrocyte size (thyrocyte area divided by number of visible nuclei), and follicle lumen area (colloid area) then analyzed. Box plot represents 5<sup>th</sup> to 95<sup>th</sup> percentiles, and horizontal line in box represents median values. Whiskers of boxes represent error bars. Data analysis was performed using Student's *t*-test with GraphPad Prism v7.0. SHJH, SHJH<sup>hr</sup> mice; ICR, ICR mice. \**P*<0.05, \*\**P*<0.01, \*\*\**P*<0.001.



**Supplementary Figure S3. Thyroid follicles in SHJH<sup>hr</sup> mice showed an increase in follicle cell number and thyrocyte area.** H&E-stained thyroid sections were used to measure follicle area, follicle lumen area, and follicle cell nuclei with ImageJ, with number of cells per follicle, thyrocyte area, and follicle lumen area (colloid area) then calculated. Box plots in A, B, and C represent 5<sup>th</sup> to 95<sup>th</sup> percentile, horizontal lines within boxes represent mean value, and error bars represent lowest and highest value in 5<sup>th</sup> percentile and 95<sup>th</sup> percentile, respectively. SHJH, SHJH<sup>hr</sup> mice; ICR, ICR mice.  $n=6$  (three male and three female mice in each group). \* $P<0.05$ , \*\*\* $P<0.001$ .



**Supplementary Figure S4. Nine-month-old SHJH<sup>hr</sup> mice showed higher T3 and T4 levels than ICR mice.** (A-C) TSH, T3, and T4 levels in 9-month-old mice ( $n=6$ ), respectively. Box plot represents 5<sup>th</sup> to 95<sup>th</sup> percentiles and horizontal lines in boxes represent medium values. Whiskers of boxes represent error bars. ICR, ICR mice; SHJH, SHJH<sup>hr</sup> mice. \* $P<0.05$ , \*\*\* $P<0.001$ .



## Supplementary Tables

**Supplementary Table S1.** *Hr* polymorphisms in SHJH<sup>hr</sup> mice

Exon	Mutant site*	Amino acid
Exon 3	1824A > G	Q303G
Exon 3	2151C > T	G412G
Exon 4	2314C > T	R467X
Exon 4	2443T > A	S510T
Exon 5	2516-2518del	G534del
Exon 6	2703T > C	S596S
Exon 19	5527T > C	

\*Mutant site refers to *Hr* mRNA sequence NM\_001379479.

**Supplementary Table S2.** Polymorphisms in mouse *Hr* gene

<b>Allele</b>	<b>Location</b>	<b>Mutant position*</b>	<b>Mutant form</b>	<b>Reference</b>
<i>hr<sup>hr</sup></i>	Intron 6	Pmv43 insertion	Mis-splicing	(Cachon-Gonzalez et al., 1999)
<i>hr<sup>rh</sup></i>	Exon 6	2704C>T	R597X	(Cachon-Gonzalez et al., 1999)
<i>hr<sup>r<sup>h</sup>sl</sup></i>	Exon 12	3648G>A	W911X	(Zhang et al., 2005)
<i>Hr<sup>r<sup>h</sup>-J</sup></i>	Exon 5	2515-2517del	E534del	(Tian et al., 2004)
<i>Hr<sup>r<sup>h</sup>-7J</sup></i>	Exon 3	1789G>A	W292X	(Cachon-Gonzalez et al., 1999)
<i>Hr<sup>r<sup>h</sup>-8J</sup></i>	Exon 4	2448-2449 GA>TT	Q511H, K512X	(Ahmad et al., 1999a)
<i>Hr<sup>r<sup>h</sup>-bmh</sup></i>	Exon 19	4456 del 296 bp	Deletion at the 3' end of hairless gene	(Brancaz et al., 2004)
<i>hr<sup>r<sup>h</sup>Chr</sup></i>	Exon 4	2314C>T	R467X	(Ahmad et al., 1999a)
<i>hr<sup>r<sup>h</sup>Y</sup></i>	Exon 16	4058 ins 13bp	Frameshift, premature stop codon at aa 1137	(Panteleyev et al., 1998a)
<i>hr<sup>r<sup>h</sup>KIZ</sup></i>	Exon 11	3355C>T	R814X	(Tian et al., 2004)
<i>hr<sup>Tg5053Mm</sup></i>	Intron 5-Exon 8	Transgene insertion	Deletion of most the 3' end of hairless gene	(Cachon-Gonzalez et al., 1999)
<i>Hr<sup>tm1Cct</sup></i>	Exon 8-10	Homologous recombination	Loss of function (hr(-/-))	(Zarach et al., 2004)
<i>Hr<sup>Ov#</sup></i>	Exon 1-19	Transgene insertion	( <i>Hr</i> gene with 3648 G>A mutant) W911X	(Zhu et al., 2017)
<i>hr<sup>SHJH</sup></i>	Exon 4	2314C>T	R467X	This report

\*Mutant sites were modified according to *Hr* mRNA sequence NM\_001379479.

#*Hr<sup>ov</sup>* is named after *Hr* gene overexpression according to (Zhu et al., 2017).

**Supplementary Table S3. Primer details**

Primer name	Sequence (5'-3')
Hr-F1	GAGTGGTCCAGCAGGCACGGG
Hr-R1	GGCGCGGTGTGGGCGGCGGTC
Hr-F2	GTACCCAGCACCGGCTAGCAC
Hr-R2	TGGTTCCTTCTGCTGACCCCC
Hr-F3	GCAAATTCCGGAGTCCGACC
Hr-R3	CCACACCGTCTAAGTTCCCC
Hr-F4	GCCCTGGCTCTAAAGGGAACA
Hr-R4	AAGGGCCATGGGGGAGGGGTC